Structural Differences Between Allelic Variants of the Ovine Prion Protein Revealed by Molecular Dynamics Simulations

Raymond Bujdoso,[1]* David F. Burke,[2] and Alana M. Thackray[1]
[1]*Centre for Veterinary Science, Department of Veterinary Medicine, University of Cambridge, Madingley Road, Cambridge, CB3 OES, UK*
[2]*Department of Biochemistry, University of Cambridge, Tennis Court Road, Cambridge, CB2 1GA, UK*

ABSTRACT **We have modeled ovine prion protein (residues 119–233) based on NMR structures of PrP from other mammalian species. Modeling of the C-terminal domain of ovine PrP predicts three helices: helix-1 (residues 147–155), flanked by two short β-strands; helix-2 (residues 176–197), and helix-3 (residues 203–229). Molecular dynamics simulations on this model of ovine PrP have determined structural differences between allelic variants. At neutral pH, limited root mean-squared (*RMS*) fluctuations were seen in the region of helix-1; between β-strand-2 and residue 171, and the loop connecting helix-2 and helix-3. At low pH, these *RMS* fluctuations increased and showed allelic variation. The extent of *RMS* fluctuation between β-strand 2 and residue 171 was ARR > ARQ > VRQ. This order was reversed for the loop region connecting helix-2 and helix-3. Although all three variants have the potential to display an extended helix at the C-terminal region of helix-1, the major influence of the VRQ allele was to restrict the conformations of the Asn162 and Arg139 side-chains. Variations observed in the simulations in the vicinity of helix-1 correlated with reactivity of C-terminal specific anti-PrP monoclonal antibodies with peripheral blood cells from scrapie-susceptible and -resistant genotypes of sheep: cells from VRQ homozygous sheep showed uniform reactivity, while cells from ARQ and ARR homozygous sheep showed variable binding. Our data show that molecular dynamics simulations can be used to determine structural differences between allelic variants of ovine PrP. The binding of anti-PrP monoclonal antibodies to ovine blood cells may validate these structural predictions. Proteins 2005;61:840–849.** © 2005 Wiley-Liss, Inc.

Key words: PrP; polymorphisms; transmissible spongiform encephalopathies; epitope; computational

INTRODUCTION

Prion diseases, such as scrapie in sheep, BSE in cattle, and CJD in humans, are transmissible chronic neurodegenerative disorders characterized by the accumulation of PrPSc, an abnormal isomer of the host protein PrPC. These two isomers of PrP are chemically indistinguishable, but differ in their secondary structures.[1–3] PrPC is predominantly α-helical (42%) with little β-sheet (3%), while PrPSc has considerably more β-sheet content (43%) and a similar α-helical content (30%).[4–6] These observations suggest that during conversion of PrPC to PrPSc, a major refolding event occurs that results in a more extensive β-sheet conformation. PrPSc is characterized by its partial resistance to proteolytic digestion and its ability to form highly insoluble aggregates while PrPC is monomeric.[7,8]

The protein-only hypothesis postulates that the transmissible prion agent consists solely of proteinaceous material.[9] Consequently, it is proposed that PrPSc forms part, or all, of the infectious prion agent, and that this abnormal isomer is responsible for the modification of the normal cellular form, PrPC. Recombinant PrP refolded under oxidizing conditions yields predominantly α-helical protein, whereas refolding under reducing conditions generates a form with a higher β-sheet content.[10,11] The β-sheet form of recombinant PrP displays characteristics similar to PrPSc, which include partial resistance to proteolytic digestion and the propensity to form insoluble amorphous aggregates.[12] Recently, a β-rich form of mouse recombinant PrP (residues 89–230) has been shown to be infectious in mice that overexpress this protein.[13,14]

Polymorphisms in ovine PrP at amino acid residues 136, 154, and 171 are associated with differences in susceptibility to natural scrapie.[15,16] Animals that express the allelic variant V136R154Q171 (VRQ) or A136R154Q171 (ARQ) show susceptibility to natural scrapie, while those with A136R154R171 (ARR) show resistance. The molecular mechanism that accounts for the variation in natural scrapie susceptibility is unknown. Clearly, critical polymorphic amino acid residues will influence the extent or stability of structural changes within ovine PrP, or its interaction with potential cofactors such as Protein X,[17,18]

Grant sponsor: BBSRC; Grant sponsor: Defra; Grant sponsor: the Wellcome Trust.

Correspondence to: Raymond Bujdoso, University of Cambridge, Centre for Veterinary Science, Department of Veterinary Medicine, Madingley Road, Cambridge, CB3 OES, UK. E-mail: rb202@cam.ac.uk

Received 22 April 2005; Revised 25 July 2005; Accepted 2 August 2005

Published online 26 October 2005 in Wiley InterScience (www.interscience.wiley.com). DOI: 10.1002/prot.20755

as it converts from the normal to disease-associated form of PrP. Several studies have investigated the biophysiochemical properties of different allelic variants of ovine recombinant PrP.[19,20] These have shown that PrP protein of the scrapie-susceptible genotypes VRQ and ARQ has a more compact structure and higher thermal denaturation temperature compared to ARR protein. Despite this difference in thermodynamic stability, all three ovine PrP genotypes can form unfolding amyloidogenic intermediates in an acidic as well as neutral environment. However, the rate of formation and β-sheet secondary structure content of the unfolding amyloidogenic intermediates are affected by the ovine PrP genetic polymorphisms, and both show a positive correlation with scrapie susceptibility.[19] Here we report for the first time the use of molecular dynamics simulations to predict the range of structural conformations adopted by scrapie-susceptible and -resistant allelic forms of ovine PrP that may account for differences in their stability and amyloidogenic potential.

Molecular dynamics simulations has allowed conformational properties of the ovine PrP protein to be determined through the generation of atomic positions as a function of time. This can be used to provide a comprehensive computational structural topography of the protein while immersed in solvent.[21,22] Our analysis showed allelic variation based on conformational fluctuations in the region of helix-1; in the region between β-strand-2 and residue 171, and in the loop connecting helix-2 and helix-3 of ovine PrP. Although all three variants have the potential to display an extended helix at the C-terminal region of helix-1, the major influence of the VRQ allele was to restrict the conformations of the Asn162 and Arg139 side-chains. The predicted structural variation in the vicinity of helix-1 correlated with the reactivity of C-terminal specific anti-PrP monoclonal antibodies with peripheral blood mononuclear cells (PBMCs) from scrapie-susceptible and -resistant genotypes of sheep. Cells from VRQ homozygous sheep showed uniform reactivity with monoclonal antibodies that bound to epitopes in the C-terminal region of helix-1, while cells from ARQ and ARR homozygous sheep showed variable binding. Collectively, our data indicate that molecular dynamics simulations can be used to predict structural differences between allelic variants of ovine PrP that are supported by in vivo and in vitro findings. We suggest that ovine PrP VRQ is a more rigid and stable structure compared to ARR, and that this difference has significant consequences for metabolism of the two proteins and their pathogenic potential.

MATERIALS AND METHODS

Comparative Modeling

Models of the C-terminal domain (residues 119–233) of ARR, ARQ, and VRQ ovine PrP were built through the use of the program MODELLER[23] using default parameters based upon the NMR or X-ray structures of human, mouse, bovine, and Syrian hamster PrP.

Details of Molecular Dynamics Simulations

The molecular dynamics simulations were carried out using the program Gromacs[24] using the OPLS-AA/L all-atom force field. The model of each allelic variant of ovine PrP was placed in an $80 \times 80 \times 80$ Å box containing 5500 water molecules, and energy minimised for 1000 steps to remove any unfavorable contacts. Molecular dynamics simulations were performed at 300K for 10 ns. The simulations were carried out using 1-s step size and the coordinates saved every 100 ps. Long-range electrostatic interactions were calculated using Particle Mesh Ewald (PME). At neutral pH (pH 7, above the pKa of histidine) glutamate and aspartate residues were negatively charged; lysine and arginine were positively charged and the histidines were neutral. To simulate low pH, the histidines were protonated at the ε position (ND1) with all other ionizable residues (aspartate and glutamate) also protonated.

Isolation of Ovine Peripheral Blood Mononuclear Cells (PBMCs) and Flow Cytometry

Peripheral blood from 3.5–4-year-old New Zealand-derived scrapie-free female Cheviot sheep was collected into EDTA tubes by venepuncture from live animals, transported on ice and routinely stored at 4°C overnight. A buffy coat was prepared by centrifugation at $733 \times g$ for 20 min at 21°C and the harvested cells were layered onto NycoPrep™ Animal (density 1.077 g/mL; osmolarity 265 mOsm), and centrifuged at $600 \times g$ for 15 min at 21°C. Mononuclear cells were recovered from the density medium interface and washed three times in FACS buffer (phosphate-buffered saline containing 1% heat-inactivated foetal calf serum plus 0.1% sodium azide) prior to immunofluorescence staining. Cell-surface phenotype was assessed using aliquots of 1×10^6 cells incubated with anti-PrP monoclonal antibody T325 or A516[25] culture supernatant, or normal mouse serum at 1/1000 as control, for 20 min at 4°C followed by three washes in FACS buffer and incubation with goat anti-mouse IgG1-biotin (Caltag, cat. no. M32115) at 1/500, for 20 min at 4°C. Cells were washed three times with FACS buffer and subsequently incubated with 0.25 μg of streptavidin–phycoerythrin (Pharmingen, cat. no. 554061) for 20 min at 4°C. Cells were finally washed three times with FACS buffer and analyzed for cell-surface fluorescence using a FACSCalibur® (Becton Dickinson, Mountain View, CA). Ten thousand cells were analyzed per sample, with dead cells excluded on the basis of forward and side light scatter.

Nomenclature

Amino acid residue numbers refer to the ovine PrP sequence.

RESULTS

Structural Features of Ovine PrP

The predicted amino acid sequences of the allelic variants ARR, ARQ, and VRQ of the ovine prion protein showed approximately 90% homology with other mammalian forms of PrP (Fig. 1). NMR structures have been described for several different mammalian forms of recombinant PrP and native bovine PrPC, and these showed common structural features, in particular within the C-terminal region of the protein.[26–31] Accordingly, we have

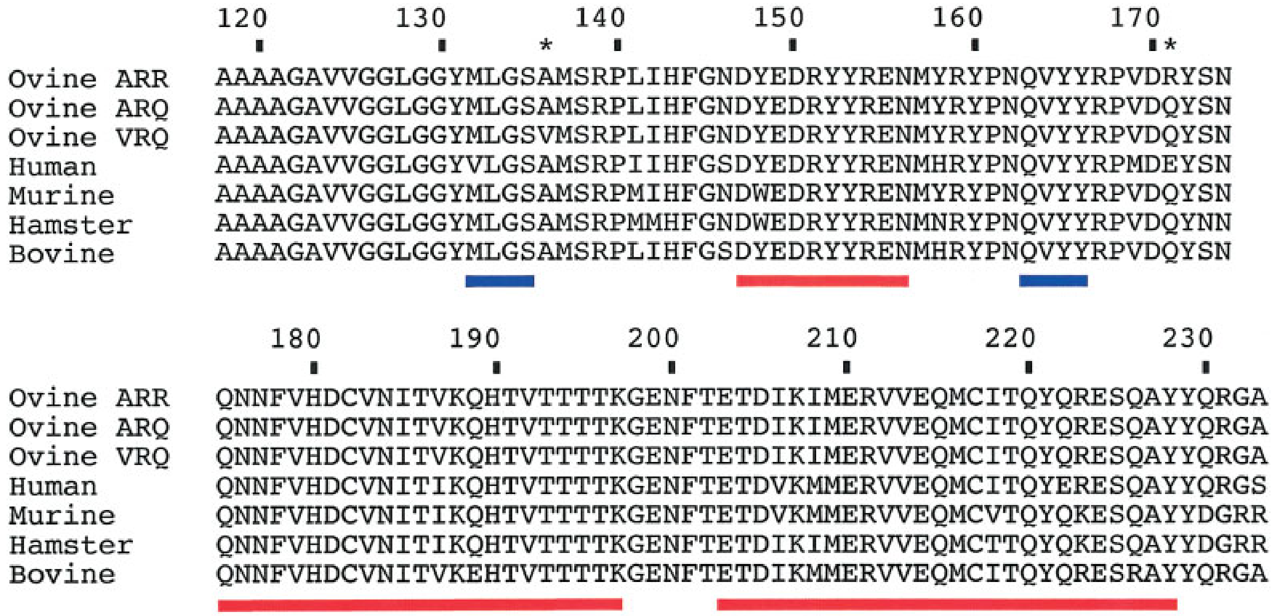

Fig. 1. Comparison of amino acid sequence in the C-terminal domain of PrP. Sequence alignment of the C-terminal domain (residues 119–233) of the ovine PrP gene with other mammalian species. Position of allelic variants 136 and 171 in ovine PrP are denoted by the asterisks. Red bar represents α-helical region; blue bar represents β-sheet region.

modeled the structure of ovine PrP (residues 119–233), incorporating an intact di-sulphide bond, based on existing NMR structures of human, mouse, bovine, and hamster PrP. Our model of the predominantly globular domain of ovine PrP predicted three helices that comprise: helix-1 (residues 147–155); helix-2 (residues 176–197), and helix-3 (residues 203–229). Helix-1 was flanked by β-strand-1 (residues 134–136) and β-strand-2 (residues 164–166). A stable di-sulphide bond was predicted between Cys182 and Cys217, which connected helix-2 and helix-3, while Asn184 and Asn200 were predicted to be N-linked glycosylation sites. These structural features of ovine PrP are shown in Figure 2, and were seen in ARR, ARQ, and VRQ allelic variants.

The structural features of ovine PrP predicted from our modeled structure were similar to those described in the recent reports that show crystal structures of the ovine prion protein, and which were published during the progress of this work.[32,33] It is noteworthy, that the crystal structures of ovine VRQ, ARQ, and ARR PrP published by Eghiaian et al. utilized amino residues 127–228 bound to a Fab moiety of an anti-PrP monoclonal antibody,[32] whereas we have modeled a longer length of the PrP polypeptide chain, namely residues 119–233. There was good agreement between our modeled structures of ovine PrP with the respective X-ray crystallographic structures of these allelic variants as shown by *RMS* deviation values of 1.2, 1.3, and 1.3 Å for ovine VRQ, ARQ, and ARR PrP, respectively. There were two regions that showed very small variations in the *RMS* deviation between the modelled and the X-ray crystallographic structures. One was in the region comprising amino acid residues 141–146. This region has extremely high thermal fluctuations, >70 $Å^2$ as measured by atomic temperature factors, indicating

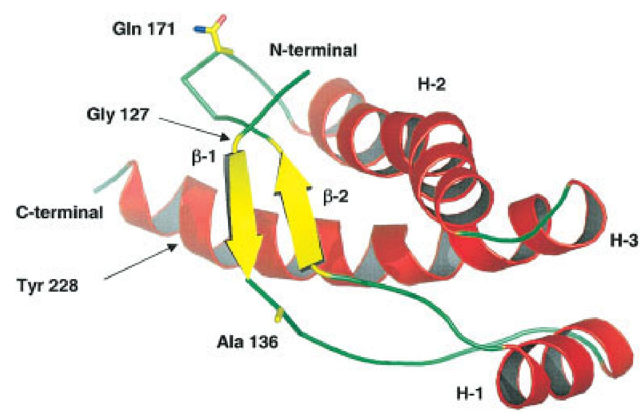

Fig. 2. Ribbon diagram of the C-terminal domain of ovine PrP-ARQ (residues 119–233). Ribbon diagram of the C-terminal domain of the ARQ allelic variant of ovine PrP. The diagram was generated using the program PyMol (DeLano, W.L. http://www.pymol.org). The sites of allelic variation Ala136 and Gln171 are shown.

uncertainty about the actual atom positions.[32] The amino acid residues in this region of PrP were also reported to have stereochemical properties that deviate from expected values. The second region was in the loop consisting of amino acid residues 171–174. This loop is the most highly variable region of all PrP structures currently solved. Accordingly, the *RMS* deviation value for our modeled structures and the X-ray crystalographic structures falls to 0.74, 0.84, and 0.81 Å for VRQ, ARQ, and ARR when the contribution of residues 141–146 and 171–174 are ignored. The accuracy of the ovine PrP crystal structures is reported to be 0.4 Å.[32] However, a recent study suggests that the limit of accuracy of X-ray structures is no less than 0.8 Å.[34] These observations clearly demonstrate the validity of

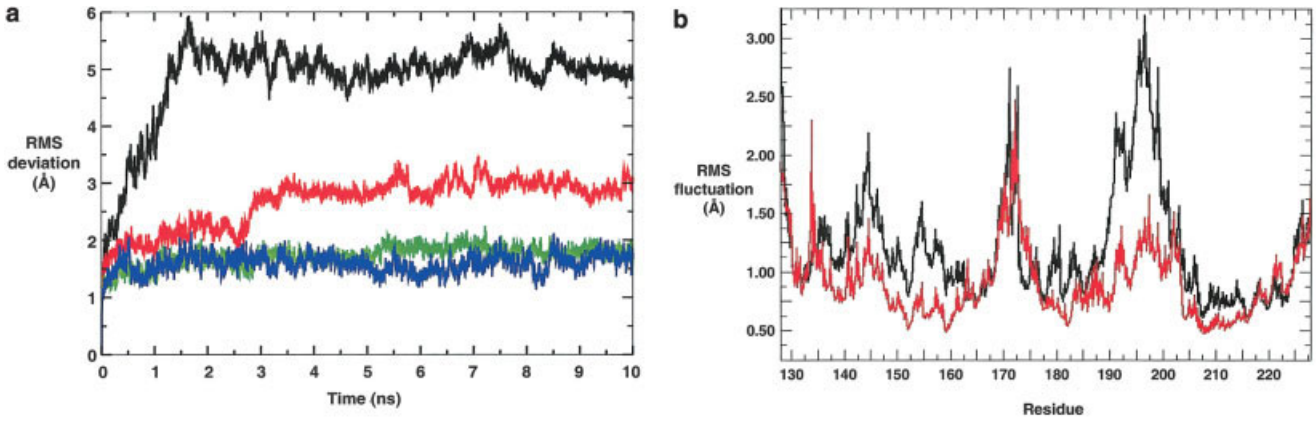

Fig. 3. Molecular dynamics simulations of ovine PrP at neutral and low pH. **(a)** Root-mean-squared (*RMS*) deviation of ovine PrP–ARQ structures from the simulations compared to the starting structure (amino acids 119–233) against time (nanoseconds) at neutral pH (red line) and low pH (black line). Also shown is the *RMS* deviation for the amino acids common to the crystal structure (127–228) at neutral pH (green line) and low pH (blue line). (**b**) RMS fluctuation of the backbone amino acids for the PrP–ARQ structures from the simulations for each residue at neutral pH (red line) and low pH (black line).

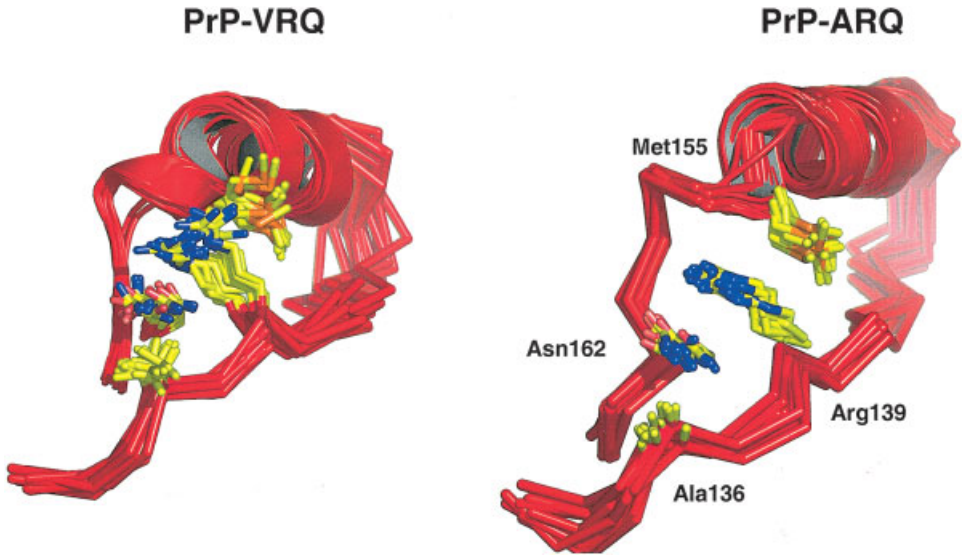

Fig. 4. Side-chain interactions around helix-1 of ovine PrP. Ribbon diagrams showing the side-chain conformations and interactions in the region of helix-1 for Ala136, Arg139, Met155, and Asn162 observed throughout the molecular dynamics simulations for ovine PrP–VRQ and PrP–ARQ at neutral pH. A representative set of 10 structures from the simulations are shown.

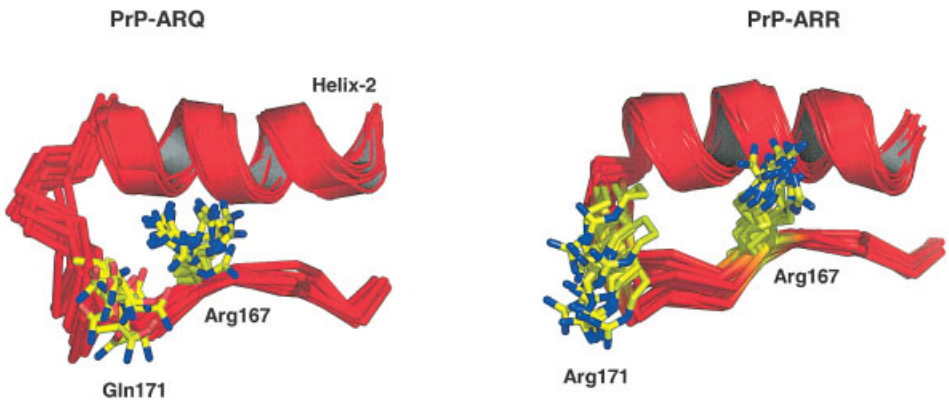

Fig. 5. Side-chain conformations of residue 171 and Arg167. Ribbon diagrams showing the side-chain conformations of residues Gln171 or Arg171 and Arg167 in ovine PrP–ARQ and PrP–ARR observed throughout the molecular dynamics simulations at neutral pH. A representative set of 10 structures from the simulations are shown.

our computational model of ovine PrP for use in the assessment of prion protein allelic structural variation.

The conversion of PrPC to PrPSc during prion disease is believed to occur in an acidic endosomal pathway and/or caveolae-like domains,[35,36] and lower pH appears to accelerate the conversion process in a cell-free assay system.[3] We have carried out molecular dynamics simulations of the modeled structure of ovine PrP, over a 10-ns time scale, at neutral and low pH to see if any significant differences in structural features occur between the allelic variants of ovine PrP under these different environmental conditions. Molecular dynamics simulations were performed on the modeled ovine PrP VRQ, ARQ, and ARR structures (residues 119–233) immersed in a box of water molecules and with an intact di-sulphide bond. Figure 3(a) shows the overall *RMS* deviation for ARQ conformations in relation to the starting structure. At neutral pH the *RMS* deviation for ovine PrP (residues 119–233) remains fairly constant at approximately 3.0 ± 0.25 Å over the measured time period. However, at low pH over the same time period, the *RMS* deviation for ovine PrP (residues 119–233) progressively increased and eventually plateaued at approximately 5.2 ± 0.5 Å. For comparison, the *RMS* deviation at neutral and low pH was established for the sequence of ovine PrP used to generate X-ray crystal structures of ARR, ARQ, and VRQ allelic variants, namely residues 127–228.[32] The *RMS* deviation for the ovine PrP peptide comprising residues 127–228 was in the region of 1.5–2 Å. This indicates that the majority of the high *RMS* deviation values seen with the ovine PrP peptide comprising residues 119–233 were clearly due to the N-terminal (residues 119–126) and C-terminal (residues 229–233) amino acids. Furthermore, this data also suggests that within the ovine PrP peptide chain comprising amino acids 119–233, residues 127–228 adopt a single conformation, irrespective of the pH environment, while the N-terminal (residues 119–126) and C-terminal (residues 229–233) amino acids show significant structural variation at low pH. All three allelic variants of ovine PrP showed similar trends as that shown for ovine PrP ARQ.

Although the molecular dynamics simulations of ovine PrP residues 119–233 suggested that the central portion of the protein adopted a single conformation, there was clear evidence of mobility throughout the polypeptide chain. The mobility of different regions of the PrP backbone was assessed by comparing *RMS* fluctuation of individual atoms within the peptide backbone at neutral and low pH, measured as mean deviation over the duration of the molecular dynamics simulations, in comparison to their position within the starting structure. Figure 3(b) shows that particular regions of ovine PrP (residues 119–233) were more mobile than others, and that this was affected by the pH of the simulation. At neutral pH, *RMS* fluctuation was seen in the region of helix-1; in the region between β-strand-2 and residue 171, and in the loop connecting helix-2 and helix-3. At low pH, the *RMS* fluctuation of these regions was amplified and showed allelic variation. The extent of *RMS* fluctuation in the region between β-strand-2 and residue 171 was ARR > ARQ > VRQ, while this order was reversed for the loop region connecting helix-2 and helix-3. These structural features were examined in our model of ovine PrP in greater detail, and the comparison of differences in allelic structures under different pH conditions are described below.

Region Between β-Strand-1 and Helix-1

When the structure of ovine VRQ was compared to that of ARQ and ARR, a significant difference was seen at the C-terminal region of helix-1 (Fig. 4). In the VRQ genotype, the α-helical structure ends at amino acid residue 155. In the ARQ and ARR genotypes residues 156–158 form a less compact 3_{10} helical structure. In this region, a network of interactions exists between Val/Ala136, Arg139, and Asn162. Most notably, there was the presence of a hydrogen bond between Asn162 and Arg139, which had been predicted by the recent crystal structure of ovine PrP.[32] In this area His143 interacted with Arg154 and Leu141. In addition, Arg139 also interacted with Tyr158 and Met157, both of which are at the end of helix-1. In VRQ, the backbone of this region of peptide containing residues 136–139 moved due to the presence of the bulkier Val136 side-chain. The position of the side-chain of Arg139 within VRQ was displaced over 4 Å relative to its position in the Ala136 structures. VRQ showed restricted backbone and side-chain movement in the region around residue 136 and interacted directly with Asn162. Additional side-chain conformations were seen with Asn162 at low pH in both ARQ and ARR that were not evident in VRQ. These differences in mobility were most probably due to the reduction in size of the side-chain in the Val136Ala polymorphism, which potentially disrupted the Asn162–Arg139 hydrogen bond. Although all three allelic variants have the potential to display an extended helix at the C-terminal region of helix-1, the major influence of the VRQ allele was to restrict the conformations of the Asn162 and Arg139 side-chains.

Region Around Residue 171

In this region of the protein, the polypeptide backbone leading up to residue 171 formed a fairly extended conformation (Fig. 5). In the Gln171 allele, the average length of β-strands-1 and -2 throughout the simulations was five and four residues, respectively. Gln171 was seen to form a hydrogen bond with the neighboring Arg167 residue approximately 30% of the time in both the ARQ and VRQ alleles. This hydrogen bond is also observed in the crystal structure of ARQ.[32] In ARQ, Gln171 had the largest *RMS* fluctuation of any of the allelic variants. This was due to the side-chain adopting many distinct conformations throughout the simulations.

The mutation of Gln171Arg caused a large movement in the backbone conformation (Fig. 5) of this region, disrupting the β-sheet formed between β-strands-1 and -2. The average length of β-strand-1 and β-strand-2 in the ARR allele was reduced by two and three residues, respectively. This movement is likely to be caused by strong charge–charge repulsion between Arg171 and Arg167. The side-

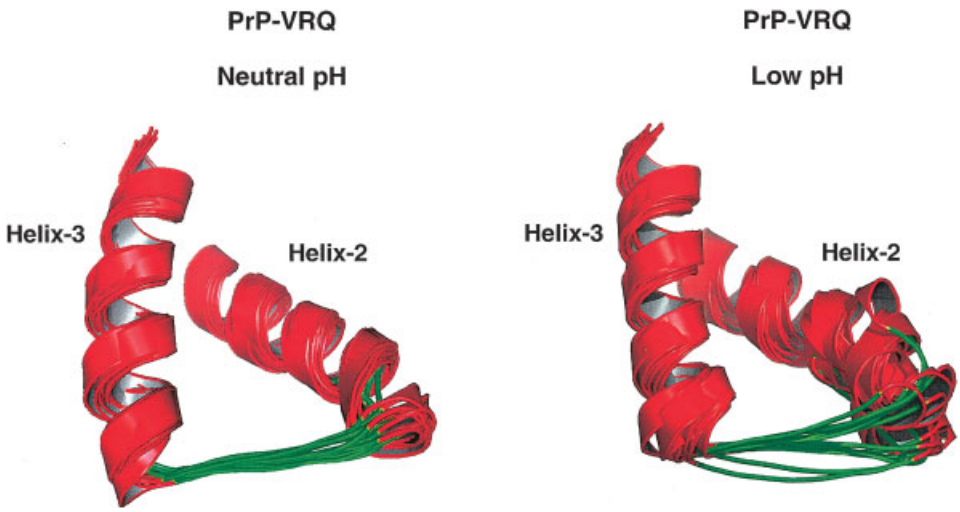

Fig. 6. Conformations of helix-2-helix-3 loop in ovine PrP. Ribbon diagrams showing the conformations adopted by the loop comprising residues 180–220 between helix-2 and helix-3 in ovine PrP throughout the molecular dynamics simulations at neutral or low pH. A representative set of 10 structures from the simulations of the VRQ allelic variant are shown.

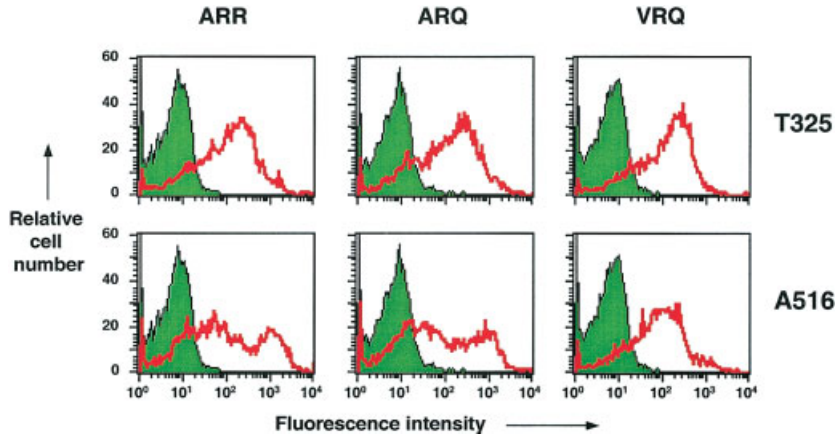

Fig. 7. Reactivity of anti-PrP monoclonal antibodies with ovine PBMCs. Ovine PBMCs from ARR, ARQ, or VRQ homozygous sheep were tested by FACS analysis as described in the Materials and Methods. Profiles shown are representative of five out of five sheep for each genotype. Upper panel: monoclonal antibody T325; lower panel: monoclonal antibody A516. Shaded peak represents control fluorescence; red line represents T325 or A516 fluorescence.

chains of both residues were pushed apart and adopted a very restricted set of conformations. This backbone flexibility was also seen at low pH for the ARQ allele. It is likely that the ARR and ARQ alleles are less stable.

Region Between Helix-2 and Helix-3

At neutral pH, the conformation of the loop connecting helix-2 and helix-3 showed little structural variation for any of the alleles. However, at low pH all of the PrP allelic variants showed large conformational changes in this loop (Fig. 6). This variation was genotype specific as the C-terminal end of helix-2 showed a greater amount of flexibility in the disease-susceptible alleles, ARQ and VRQ, whereas the disease-resistant allele ARR showed a greater amount of structural variation at the middle of the loop, especially around residue Glu199.

Structural Differences Between Allelic Forms of Cell-Surface Ovine PrPC

The molecular dynamics simulations data predicted that a major area of conformational variation existed between Ala136 and Val136 genotypes of ovine PrP in the C-terminal region of helix-1. It was shown that in the VRQ allelic variant, Val136 restricted the movement of amino acids in this area favoring the formation of a hydrogen bond between Asn162 and Arg139. In contrast, the presence of Ala136 allowed more structural flexibility in this region. We investigated this predicted structural variation in the Ala136 genotypes of ovine PrP by probing the conformation of ovine cell-surface PrPC with anti-PrP monoclonal antibody A516, which recognizes an epitope in the C-terminal region of helix-1.[25] Although monoclonal antibody A516 was reactive with ovine cell-surface PrPC,

there was considerable heterogeneity when reacted with PBMCs from sheep of different genotypes. Figure 7 shows that this monoclonal antibody reacted with all PBMCs from VRQ homozygous sheep and with a reactivity profile that was typically a single peak. In contrast, cells from ARR and ARQ homozygous sheep typically showed two populations of cells; one that displayed relatively low fluorescence intensity with monoclonal A516 and a second that expressed the A516 epitope with a similar intensity to that seen with cells from VRQ sheep. All of the PBMCs from all three genotypes of sheep expressed PrPC as shown by their reactivity with the N-terminal-specific anti-PrP monoclonal antibody T325, which reacted with a similar level of intensity with all cells (Fig. 7). Therefore, the variation in monoclonal antibody A516 binding to cells of the ARR and ARQ genotype would not appear to be due to genotypic differences in cell-surface PrPC expression levels. Collectively, these data indicate that Ala136 cell-surface PrPC displays greater structural variation than does the Val136 genotypic form of this protein in the C-terminal region of helix-1, as indicated by molecular dynamics simulations.

DISCUSSION

The NMR structures of PrP from a variety of different mammalian species have now been described, as well as crystal structures of the globular domain of human and ovine PrP.[26–33,37] In all of the species investigated so far, PrP consists of a flexible N-terminal region comprising ≈ 100 amino acids followed by a globular C-terminal region of ≈ 100 amino acids. Computational modeling has allowed us to determine that the structure of the C-terminal domain of ovine PrP comprises three α-helices, interdispersed by a short antiparallel β-sheet region similar to that described for other species forms of PrP. There is a close association between helix-1, the C-terminal region of helix-2, and the N-terminal region of helix-3, and this central core is bound by an intramolecular di-sulphide bond between residues 182 and 217. Our computational model of ovine PrP shows a good correlation with the crystal structures of ovine PrP that were reported during the progression of the studies reported here.[32,33] In particular, the *RMS* deviation between our computational model of ovine PrP and the crystal structures of ovine PrP, over those residues that are common between both, show values of <1.0 for all of the allelic variants tested. The major polymorphisms in ovine PrP associated with differences in susceptibility to natural scrapie in sheep occur in the C-terminal portion of the molecule at amino acid residues 136, 171, and to a lesser extent, 154. These polymorphic residues are located on the surface of the protein and their side-chains are water exposed. All three polymorphic sites are located within, or close to, that region of PrP that undergoes the major conformational change associated with conversion of PrPC to PrPSc during prion disease.[38] Inspection of the modeled structure of ovine PrP reported here shows that two of the major polymorphic amino acid positions, residues 136 and 171, are spatially quite close and occur on either side of the β-strands that flank helix-1. Substitutions at both of these sites, appears to influence the structural composition of this central region of the protein and the overall stability of the molecule.

Our computational modeling of ovine PrP shows the Ala136Val polymorphism is likely to result in an increase in the β-sheet content of PrP. Valine, a β-sheet former, will extend β-strand-1 and its bulkier side-chain restricts the movement of the Asn162 and Arg139 side-chains, with the resultant loss of potential to display an extended helix at the C-terminal region of helix-1. These structural features are further enhanced by the effect of the Arg171Gln polymorphism, which results in a decrease in the flexibility of the polypeptide backbone leading up to residue 171, and an increase in the length of both β-strand-1 and β-strand-2. In addition, while a hydrogen bond is seen between Gln171 and Arg167, this is not present in the ARR allele. The resultant loss of β-strand length and loss of a hydrogen bond between residues 171 and 167 collectively results in the loss of stability of the β-sheet region and probably to a loss in the potential for β-sheet formation in the Arg171 allele. These data support the hypothesis that polymorphisms in ovine PrP have a significant affect upon the secondary structure of the protein. This is also suggested by our recent observations, which show that after copper treatment of ovine PrP, the VRQ allelic form displays a greater increase in β-sheet content than does the ARR allelic form, which remains relatively structurally unchanged.[20] Furthermore, our data reported here have shown that residues 119–126 of ovine PrP have the highest variability and mobility throughout the molecular dynamics simulations of peptide 119–233, and displayed pH and allele-specific differences in their conformational variation. The fact that polymorphisms in ovine PrP have local and long-range structural affects, including those upon N-terminal amino acid residues, may suggest the involvement of residues 119–126 in the formation of disease-associated PrP. It has been suggested that β-strand-1 and β-strand-2 form the basis of the β-sheet region in PrPSc, and that this region contributes to the stabilisation of this PrP isoform.[32] It has been further suggested that this region is involved in protofibril formation with β-strand-2 from one monomer forming an extended β-sheet with β-strand-1 and the N-terminal residues 114–127 from another monomer.[22,39] The extensive flexibility seen in our molecular dynamics simulations of residues 119–126 suggests that this region of PrP has sufficient mobility and structural variation to fulfil this proposed role. Further studies are warranted on the structural effects of polymorphisms on this region of ovine PrP molecules ability to form a β-sheet structure to further understand scrapie susceptibility and resistance.

Despite the extensive flexibility within the N-terminal region of PrP, the ovine prion protein displays considerable stability considering the structured C-terminal globular domain comprises approximately 100 amino acids.[19] Other proteins of similar domain length display lower ΔG^0 values. The increased stability of ovine PrP may reflect a significant contribution by the N-terminal region of the

protein to overall folding of the C-terminal domain. The Ala136Val and Arg171Gln polymorphisms modulate the stability of ovine PrP. The Ala136Val polymorphism is associated with increased ΔG^0 values, which reflect a more stable native state structure for Val136 protein compared to Ala136, in particular at low pH.[19] The Ala136Val polymorphism causes the Asn162 side-chain carbonyl oxygen to rotate, and in VRQ, results in a hydrogen bond with residue Arg139, which stabilizes VRQ compared to ARQ.[32] In contrast, the Gln171Arg polymorphism destabilizes the native state of Arg171 compared to Gln171 protein. In addition, within the ARQ allelic variant there is a hydrogen bond between residues Arg167 and Gln171. Gln171Arg polymorphism displaces the Arg167 side-chain because of electrostatic repulsion between two guanidinium groups. As a consequence, the loss of the hydrogen bond in the ARR molecule results in its destabilization compared to ARQ and VRQ,[19] which most likely leads to destabilization of the junction between β-strand-2 and helix-2. These structural changes render the scrapie-resistant allelic variant ARR destabilized compared to the susceptible alleles ARQ and VRQ. The reasons for these allelic specific differences are not clear, but it is likely to be due to a combination of long-range interactions and differences in the structural variability of each allele. The measured free enthalpy changes associated with Ala136Val and Gln171Arg mutations, are in the order of −5.9 and 4.9 kJ/mol, respectively, and are within the range of those observed when a hydrogen bond is lost or gained in a protein.[32] In addition to the affect on overall stability, the Ala136Val and Gln171Arg polymorphisms also modulate the rate of heat-induced unfolding intermediate formation and the structure of the unfolding intermediate.[19] The ARQ and VRQ allelic variant unfolding intermediates display β-sheet structure while those of the ARR genotype adopt more random coil. These data suggest that polymorphisms in ovine PrP not only affect the stability of the molecule but also its amyloidogenic potential.[19,32]

The effect of the Val136Ala polymorphism on the structural variation in the C-terminal region of helix-1 of ovine PrP predicted by the molecular dynamics simulations shown here was supported by the variation in cell-surface PrPC epitope exposure on blood cells from Ala136 and Val136 sheep. FACS profiles for blood cells from sheep of the Ala136 genotype showed at least two populations of cells with respect to reactivity with the anti-PrP monoclonal antibody A516, which binds to PrP in the C-terminal region of helix-1.[25] In contrast, cells from Val136 sheep showed only a single reactivity profile with monoclonal antibody A516. Because all of the blood cells from Ala136 and Val136 sheep expressed cell-surface PrPC as seen by their reactivity with the N-terminal-specific monoclonal antibody T325, the biphasic nature of the FACS profiles obtained with monoclonal antibody A516 on cells from the Ala136 genotype of sheep implied that distinct populations of blood cells from these animals expressed different conformations of cell-surface PrPC. The reason for this difference in PrPC conformation adopted by different blood cells of the Ala136 genotype remains to be established. Our molecular dynamics simulations data presented here clearly identified ovine PrP ARR and ARQ as more flexible in their conformational repertoire than VRQ protein, and this appears to have been reflected in the different FACS profiles obtained with cells from sheep of these genotypes. Collectively, these data indicate that heterogeneity exists within the central portion of the protein between allelic variants of cell-surface ovine PrPC. We speculate that the different FACS profiles seen with monoclonal antibody A516 are due to conformational variation around the C-terminal region of helix-1 as predicted by the molecular dynamics simulations.

The conformation adopted by cell-surface PrPC may be influenced by the membrane environment in which the protein is located. PrPC is retained on the cell-surface in sphingolipid rafts from where it is constitutively endocytosed via caveolae[36] or via clathrin-coated pits[40] by a Cu^{2+}-activated mechanism.[41–43] To be endocytosed, PrPC is believed to migrate from the detergent-insoluble "raft" environment to cluster in the nonraft membrane. Raft sphingolipids are extensively glycosylated and present a hydrophilic glycocalx above the membrane that would contribute to stabilization of the hydrophilic, α-helical form of PrPC. In contrast, the membrane surface outside rafts is dominated by nonglycosylated phosphatidylcholine that presents a more hydrophobic face to membrane proteins. As PrPC trafficks through these two biochemically distinct membrane compartments there may be very different consequences for its conformation or stability. This is supported by the fact that PrPC is resistant to conversion to PrPSc when in lipid rafts[44] and inhibition of sphingolipid synthesis enhances the conversion process.[45] This suggests that the native conformation of PrPC is protected within the lipid rafts, and remains flexible while it is in the endocytic compartment. It will be of interest to determine the phenotype of those cells that fail to express the A516 epitope, as these may locate PrPC predominantly outside of lipid rafts and have the highest potential to metabolize PrP of the Ala136 genotype.

Because VRQ is more thermodynamically stable than ARR, the disease-susceptible allelic form is likely to be characterized by a longer cellular half-life. The longer time for cellular trafficking, together with its greater resistance to protease digestion,[19] will allow VRQ a greater potential to display its pathogenic properties. The fact that the VRQ allelic variant is predisposed to more β-sheet formation compared with ARR,[20] renders the protein more susceptible to accumulate in the cell in a disease-associated form. This would support the view that differences in the metabolism of allelic variants of ovine PrP contribute to the mechanism(s) that determine susceptibility and resistance of sheep to natural scrapie.[19,32] In such a scheme, the thermodynamically less stable ARR allelic variant would be efficiently metabolized before it was able to accumulate in any significant amount in a disease-associated form. However, the ARR genotype does not confer total resistance to TSE disease because ARR homozygous sheep are susceptible to experimental prion infection, at least by direct inoculation into the CNS.[46] This would

suggest that the resistance to natural scrapie infection in ARR sheep occurs at a peripheral location. One possible site is within cells of the lymphoreticular system, either through the ability of cells to metabolize PrP or the failure of cells to produce disease-associated PrP.

Collectively, our data indicate that molecular dynamics simulations can be used to predict structural differences between allelic variants of ovine PrP. The validity of this approach was authenticated by the experimentally observed differences in anti-PrP monoclonal antibodies binding to the C-terminal region of helix-1 of different allelic forms of cell-surface ovine PrPC. This region appears to be quite flexible within the ovine PrP protein, and represents part of the central portion of PrP that undergoes the major conformational change during the conversion of PrPC to PrPSc in scrapie disease. The presence of valine, a β-sheet former, at residue 136 is likely to influence the formation of more prominent β-strand secondary structure in this area compared to the presence of alanine, an α-helix former, at the same amino acid position. The consequence of this appears to be a more rigid and stable structure in the VRQ allelic variant, compared to ARR. It is predictable that this increased stability of the VRQ protein leads to a greater resistance of either normal or disease-associated PrP to metabolism, and hence, its greater propensity to accumulate within cells.

ACKNOWLEDGMENTS

We thank ADAS, UK, for the generous supply of sheep blood.

REFERENCES

1. Caughey B, Raymond GJ. The scrapie-associated form of PrP is made from a cell surface precursor that is both protease- and phospholipase-sensitive. J Biol Chem 1991;266:18217–18223.
2. Kocisko DA, Come JH, Priola SA, Chesebro B, Raymond GJ, Lansbury PT, Caughey B. Cell-free formation of protease-resistant prion protein. Nature 1994;370:471–474.
3. Kocisko DA, Priola SA, Raymond GJ, Chesebro B, Lansbury PT, Jr, Caughey B. Species specificity in the cell-free conversion of prion protein to protease-resistant forms: a model for the scrapie species barrier. Proc Natl Acad Sci USA 1995;92:3923–3927.
4. Caughey BW, Dong A, Bhat KS, Ernst D, Hayes SF, Caughey WS. Secondary structure analysis of the scrapie-associated protein PrP 27–30 in water by infrared spectroscopy. Biochemistry 1991;30: 7672–7680.
5. Pan KM, Baldwin M, Nguyen J, Gasset M, Serban A, Groth D, Mehlhorn I, Huang Z, Fletterick RJ, Cohen FE, et al. Conversion of alpha-helices into beta-sheets features in the formation of the scrapie prion proteins. Proc Natl Acad Sci USA 1993;90:10962–10966.
6. Pergami P, Bramanti E, Ascoli GA. Structural dependence of the cellular isoform of prion protein on solvent: spectroscopic characterization of an intermediate conformation. Biochem Biophys Res Commun 1999;264:972–978.
7. McKinley MP, Meyer RK, Kenaga L, Rahbar F, Cotter R, Serban A, Prusiner SB. Scrapie prion rod formation in vitro requires both detergent extraction and limited proteolysis. J Virol 1991;65:1340–1351.
8. Prusiner SB, McKinley MP, Bowman KA, Bolton DC, Bendheim PE, Groth DF, Glenner GG. Scrapie prions aggregate to form amyloid-like birefringent rods. Cell 1983;35:349–358.
9. Prusiner SB. Novel proteinaceous infectious particles cause scrapie. Science 1982;216:136–144.
10. Lu BY, Chang JY. Isolation of isoforms of mouse prion protein with PrP(SC)-like structural properties. Biochemistry 2001;40: 13390–13396.
11. Zhang H, Stockel J, Mehlhorn I, Groth D, Baldwin MA, Prusiner SB, James TL, Cohen FE. Physical studies of conformational plasticity in a recombinant prion protein. Biochemistry 1997;36: 3543–3553.
12. Baskakov IV, Legname G, Baldwin MA, Prusiner SB, Cohen FE. Pathway complexity of prion protein assembly into amyloid. J Biol Chem 2002;277:21140–21148.
13. Legname G, Baskakov IV, Nguyen HO, Riesner D, Cohen FE, DeArmond SJ, Prusiner SB. Synthetic mammalian prions. Science 2004;305:673–676.
14. Legname G, Nguyen HO, Baskakov IV, Cohen FE, Dearmond SJ, Prusiner SB. Strain-specified characteristics of mouse synthetic prions. Proc Natl Acad Sci USA 2005;102:2168–2173.
15. Clouscard C, Beaudry P, Elsen JM, Milan D, Dussaucy M, Bounneau C, Schelcher F, Chatelain J, Launay JM, Laplanche JL. Different allelic effects of the codons 136 and 171 of the prion protein gene in sheep with natural scrapie. J Gen Virol 1995;76: 2097–2101.
16. Goldmann W, Hunter N, Smith G, Foster J, Hope J. PrP genotype and agent effects in scrapie: change in allelic interaction with different isolates of agent in sheep, a natural host of scrapie. J Gen Virol 1994;75:989–995.
17. Perrier V, Kaneko K, Safar J, Vergara J, Tremblay P, DeArmond SJ, Cohen FE, Prusiner SB, Wallace AC. Dominant-negative inhibition of prion replication in transgenic mice. Proc Natl Acad Sci USA 2002;99:13079–13084.
18. Zulianello L, Kaneko K, Scott M, Erpel S, Han D, Cohen FE, Prusiner SB. Dominant-negative inhibition of prion formation diminished by deletion mutagenesis of the prion protein. J Virol 2000;74:4351–4360.
19. Rezaei H, Choiset Y, Eghiaian F, Treguer E, Mentre P, Debey P, Grosclaude J, Haertle T. Amyloidogenic unfolding intermediates differentiate sheep prion protein variants. J Mol Biol. 2002;322: 799–814.
20. Wong E, Thackray AM, Bujdoso R. Copper induces increased beta-sheet content in the scrapie-susceptible ovine prion protein PrPVRQ compared with the resistant allelic variant PrPARR. Biochem J 2004;380:273–282.
21. Alonso DO, Daggett V. Simulations and computational analyses of prion protein conformations. Adv Protein Chem 2001;57:107–137.
22. Alonso DO, DeArmond SJ, Cohen FE, Daggett V. Mapping the early steps in the pH-induced conformational conversion of the prion protein. Proc Natl Acad Sci USA 2001;98:2985–2989.
23. Sali A, Blundell TL. Comparative protein modelling by satisfaction of spatial restraints. J Mol Biol 1993;234:779–815.
24. Lindahl E, Hess B, van der Spoel D. GROMACS 3.0: a package for molecular simulation and trajectory analysis. J Mol Model 2001;7: 306–317.
25. Thackray AM, Yang S, Wong E, Fitzmaurice TJ, Morgan-Warren RJ, Bujdoso R. Conformational variation between allelic variants of cell-surface ovine prion protein. Biochem J 2004;381:221–229.
26. Lopez Garcia F, Zahn R, Riek R, Wuthrich K. NMR structure of the bovine prion protein. Proc Natl Acad Sci USA 2000;97:8334–8339.
27. Zahn R, Liu A, Luhrs T, Riek R, von Schroetter C, Lopez Garcia F, Billeter M, Calzolai L, Wider G, Wuthrich K. NMR solution structure of the human prion protein. Proc Natl Acad Sci USA 2000;97:145–150.
28. Riek R, Hornemann S, Wider G, Billeter M, Glockshuber R, Wuthrich K. NMR structure of the mouse prion protein domain PrP(121–321). Nature 1996;382:180–182.
29. Riek R, Hornemann S, Wider G, Glockshuber R, Wuthrich K. NMR characterization of the full-length recombinant murine prion protein, mPrP(23–231). FEBS Lett 1997;413:282–288.
30. Donne DG, Viles JH, Groth D, Mehlhorn I, James TL, Cohen FE, Prusiner SB, Wright PE, Dyson HJ. Structure of the recombinant full-length hamster prion protein PrP(29–231): the N terminus is highly flexible. Proc Natl Acad Sci USA 1997;94:13452–13457.
31. Hornemann S, Schorn C, Wuthrich K. NMR structure of the bovine prion protein isolated from healthy calf brains. EMBO Rep 2004;5:1159–1164.
32. Eghiaian F, Grosclaude J, Lesceu S, Debey P, Doublet B, Treguer E, Rezaei H, Knossow M. Insight into the PrPC→PrPSc conversion from the structures of antibody-bound ovine prion scrapie-susceptibility variants. Proc Natl Acad Sci USA 2004;101:10254–10259.
33. Haire LF, Whyte SM, Vasisht N, Gill AC, Verma C, Dodson EJ,

Dodson GG, Bayley PM. The crystal structure of the globular domain of sheep prion protein. J Mol Biol 2004;336:1175–1183.
34. Eyal E, Gerzon S, Potapov V, Edelman M, Sobolev V. The limit of accuracy of protein modeling: influence of crystal packing on protein structure. J Mol Biol 2005;351:431–442.
35. Kaneko K, Vey M, Scott M, Pilkuhn S, Cohen FE, Prusiner SB. COOH-terminal sequence of the cellular prion protein directs subcellular trafficking and controls conversion into the scrapie isoform. Proc Natl Acad Sci USA 1997;94:2333–2338.
36. Vey M, Pilkuhn S, Wille H, Nixon R, DeArmond SJ, Smart EJ, Anderson RG, Taraboulos A, Prusiner SB. Subcellular colocalization of the cellular and scrapie prion proteins in caveolae-like membranous domains. Proc Natl Acad Sci USA 1996;93:14945–14949.
37. Knaus KJ, Morillas M, Swietnicki W, Malone M, Surewicz WK, Yee VC. Crystal structure of the human prion protein reveals a mechanism for oligomerization. Nat Struct Biol 2001;8:770–774.
38. Bossers A, Belt P, Raymond GJ, Caughey B, de Vries R, Smits MA. Scrapie susceptibility-linked polymorphisms modulate the in vitro conversion of sheep prion protein to protease-resistant forms. Proc Natl Acad Sci USA 1997;94:4931–4936.
39. DeMarco ML, Daggett V. From conversion to aggregation: protofibril formation of the prion protein. Proc Natl Acad Sci USA 2004;101:2293–2298.
40. Sunyach C, Jen A, Deng J, Fitzgerald KT, Frobert Y, Grassi J, McCaffrey MW, Morris R. The mechanism of internalization of glycosylphosphatidylinositol-anchored prion protein. EMBO J 2003;22:3591–3601.
41. Harris DA. Cellular biology of prion diseases. Clin Microbiol Rev 1999;12:429–444.
42. Brown DR. Prion and prejudice: normal protein and the synapse. Trends Neurosci 2001;24:85–90.
43. Prado MA, Alves-Silva J, Magalhaes AC, Prado VF, Linden R, Martins VR, Brentani RR. PrPc on the road: trafficking of the cellular prion protein. J Neurochem 2004;88:769–781.
44. Baron GS, Wehrly K, Dorward DW, Chesebro B, Caughey B. Conversion of raft associated prion protein to the protease-resistant state requires insertion of PrP-res (PrP(Sc)) into contiguous membranes. EMBO J 2002;21:1031–1040.
45. Naslavsky N, Shmeeda H, Friedlander G, Yanai A, Futerman AH, Barenholz Y, Taraboulos A. Sphingolipid depletion increases formation of the scrapie prion protein in neuroblastoma cells infected with prions. J Biol Chem 1999;274:20763–20771.
46. Houston F, Goldmann W, Chong A, Jeffrey M, Gonzalez L, Foster J, Parnham D, Hunter N. Prion diseases: BSE in sheep bred for resistance to infection. Nature 2003;423:498.